Available online at www.scholarsresearchlibrary.com

Scholars Research Library

Archives of Applied Science Research, 2011, 3 (2):107-120

(http://scholarsresearchlibrary.com/archive.html)

ISSN 0975-508X
CODEN (USA) AASRC9

Heat Sink Design and Temperature Distribution Analysis for Millimeter Wave IMPATT Oscillators using Finite Difference Method

Aritra Acharyya and J. P. Banerjee

Institute of Radio Physics and Electronics, University of Calcutta, Kolkata, India

---

ABSTRACT

Optimum Heat sink design is extremely essential for proper operation of IMPATT diode oscillators. For steady and safe operation of the oscillator without burn-out of the device, properly designed heat sink must be provided. In this paper authors have presented a new method for getting optimum designs of heat sinks capable of serving the above purpose. Moreover analytical solution of the Laplace equation for steady state heat transfer problems with proper boundary conditions for arbitrary geometries is sometime very difficult to find out. That is why numerical techniques like Finite Difference Method [FDM] can be used as very useful tool by which the solutions can be found out easily without much computational error. In this work authors have applied Finite-Difference Method to find out 2-D Temperature Distribution inside the ordinary mesa diode as well as ring diode mounted on semi-infinite diamond and copper heat sinks. Results are presented in the form of plots and tables useful for design.

Keywords: Finite Difference Method, Heat Sink, IMPATT diodes, Junction Temperature, Laplace equation, Temperature Distribution, Thermal Resistance.

INTRODUCTION

It is well known that the efficiency of the IMPATT diode is relatively low [practically 5-15% for CW operation], a large fraction of the dc power is dissipated as heat in the high-field region. The temperature of the junction rises above ambient, and in many cases output power of oscillator is limited by the rate at which heat can be extracted from the device. As junction temperature increases, the reverse saturation current rises exponentially and eventually leads to *thermal runway phenomenon* resulting the burning out of the device. Since in contrast to the avalanche current, the reverse saturation current does not require a large voltage to sustain it, the voltage begins to decrease when the junction gets hot enough for the reverse current to constitute a significant fraction of the total current. A thermally induced dc negative resistance is produced, causing the current to concentrate in the hottest part of the diode. As well as leading to the eventual burn-out of the junction, the increased saturation current at elevated temperatures

produces degradation in the oscillator performance at power levels below the burn-out value. The increased reverse saturation current produces a faster build-up of the avalanche current and degrades the negative resistance of the device. Thus, in general, the oscillator efficiency will begin to decrease at power levels just below the burn-out power. As the band-gap of the semiconductor becomes larger the reverse saturation current associated with it becomes smaller and consequently the burn-out temperature of the junction rises. Thus Ge-IMPATTs (E_g = 0.7 eV) are lower power devices than either Si (E_g = 1.12 eV) or GaAs (E_g = 1.43 eV) devices.

An immense number of analytical solutions for conduction heat-transfer problems have been accumulated in the literature over past 100 years. Even so, in many practical situations the geometry or boundary conditions are such that an analytical solution has not been obtained at all, or if the solution has been developed, it involves such a complex series solution that numerical evaluation becomes exceedingly difficult. For such situations the most fruitful approach to the problem is one based on Finite-Difference techniques. In this paper 2-Dimensional Temperature Distributions inside the DDR Continuous Wave (CW) ordinary mesa and ring diodes (Silicon-IMPATT Diodes) mounted on semi-infinite heat sink have been determined by using FDM. This approach is much easier than the analytical approach with appreciable accuracy.

The rest of this paper is organized as follows. Section 2 describes the design of W-Band continuous wave DDR Si-IMPATT diode by computer simulation method. Section 3 provides the method for determining total thermal resistances as well as junction temperatures of both mesa and ring diodes along with heat sinks. Section 4 gives a brief about the basic Finite Difference Method. In Section 5 details about the heat sink design methodology is described. How to find the temperature distribution inside the diode and heat sinks using FDM are also explained in Section 5. Results are provided in this section in terms of necessary plots and tables. Finally the paper concludes in Section 6.

Table 1. Diode structural and doping parameters

PARAMETER	VALUE
Diode Structure	Flat-DDR
Base Material	Silicon
n-epitaxial layer thickness (μm)	0.4200
p-epitaxial layer thickness (μm)	0.3800
n-epitaxial layer doping concentration ($\times 10^{23}$ m^{-3})	1.000
p-epitaxial layer doping concentration ($\times 10^{23}$ m^{-3})	1.500
n+-substrate layer doping concentration ($\times 10^{26}$ m^{-3})	1.000

Table 2. Simulated DC and Small-Signal Parameters

Bias Current Density, J_{dc} [Amp/m^2]	Peak Electric Field, E_m [V/m]	Breakdown Voltage, V_{dc} [Volts]	Efficiency, η%	Negative Resistance at Peak Freq. [Ohm]	Quality Factor, Q	Peak Operating Frequency, f_{opt} [GHz]	RF Output Power (Watt)
4.5×10^8	5.78×10^7	28.28	13.61	-1.0678	- 1.27	95	0.3421
4.8×10^8	5.75×10^7	28.38	12.81	-1.3489	-1.19	101	0.3679
5.2×10^8	5.73×10^7	28.62	12.05	-1.6954	-1.10	110	0.4211
5.5×10^8	5.71×10^7	28.86	11.20	-2.7849	-1.05	119.5	0.4328

Design of W-Band Continuous Wave Silicon DDR IMPATT Diodes

A double iterative field maximum computer method has been developed which solves the basic device equations (e.g. Poisons Equation, Current Density Equations and Current Continuity Equations) simultaneously, considering the mobile space charge effect. Detail of this method is already published elsewhere [10]. This computer program is used to design a Silicon based CW DDR IMPATT diode and optimized its performance to properly operate in W-Band. Doping and structural parameters of that designed diode is listed in Table 1. Simulated DC and high frequency Small-Signal properties for four different current densities are listed in Table 2.

Determination of Thermal Resistance and Junction Temperature

For proper operation of the diode in (CW) steady state properly designed heat sink must be attached just below the diode to avoid the thermal runway phenomenon i.e. the burn-out of the device. Heat sinks can be made of diamond or copper. In our work, we have designed heat sinks by using both diamond and copper for both ordinary mesa and ring structure of Si-IMPATT diodes. Since the thermal conductivity of diamond (k_C = 2000 watt/m ^oC) is much higher than copper (k_{Cu} = 396 watt/m ^oC); Thus to get equivalent (almost equal) junction temperatures for both the diode structures dimensions of the diamond heat sinks will be much smaller than the copper heat sinks. Figure 1(a) & (b) shows the actual structures of mesa and ring diodes over diamond/copper heat sinks. Total thermal resistances [Diode (below the junction) + Heat Sink] are determined for both mesa and ring structures by using (1) and (2). Here the p-n junctions of the both diodes are assumed as the heat source. Temperature is assumed to be distributed uniformly throughout the junction.

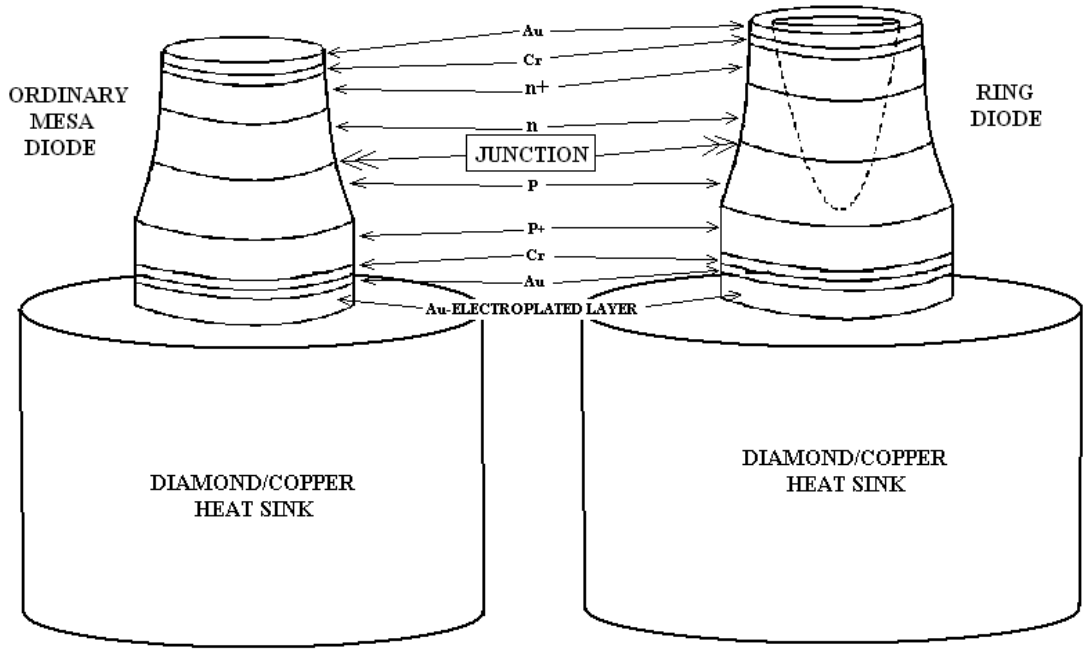

Figure 1(a) & (b): Actual Structures of Ordinary Mesa diode and Ring Diode over Semi-Infinite Diamond/Copper Heat Sink.

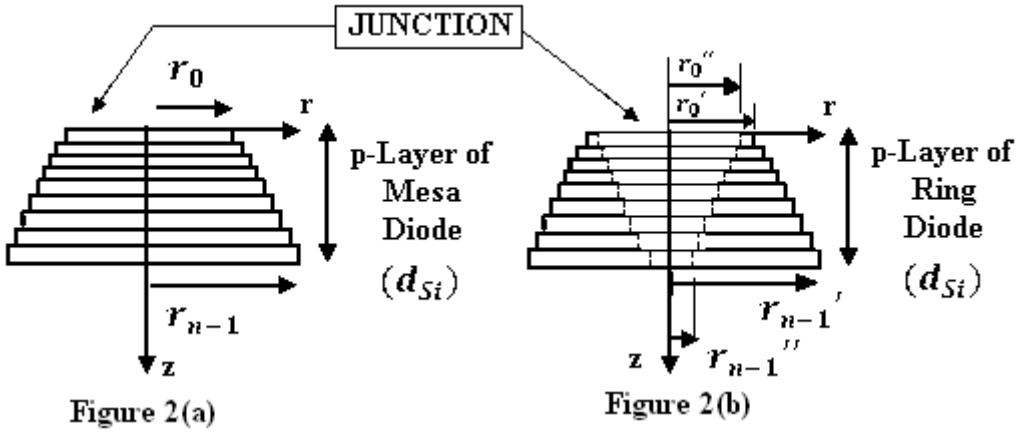

Figure 2(a) & (b): Approximations for p-Layers of both mesa and ring structures of Si-IMPATT diodes.

To determine the total thermal resistances some assumptions have been made (Figure 2(a) & (b)). Silicon *p*-layer of ordinary mesa diode is approximated as 'n' number of concentric cylinders having same axial length ($W = d_{Si}/n$) but increasing radius from 'r_0' to 'r_{n-1}' (Figure 2(a)). As number of such cylinders (n) increases, the approximation comes closer to the actual structure (Figure 1(a)). Similarly Silicon *p*-layer of ring diode is approximated as 'n' number of concentric rings having same thicknesses ($W = d_{Si}/n$) but increasing outer radius from 'r_0'' to 'r_{n-1}'' and decreasing inner radius from 'r_0''' to 'r_{n-1}''' ($r_{n-1}'' \approx 0$) from the junction towards the end of this layer (Figure 2(b)). As number of such rings increases, the approximation comes closer to the actual structure (Figure 1(b)). p^+, Cr, Au-layers together are approximated as a cylinder of fixed radius (both for mesa and ring diodes). Generally p^+, Cr, Au -layers are of square cross-section, but in our analysis [for simplicity] these are approximated as circular cross-sections. Heat sinks are also assumed as having circular cross sections.

Total thermal resistance of mesa diode [below the junction] along with the heat sink is calculated following the above assumptions using (1),

$$Rth = RSi + \frac{1}{\pi r_{n-1}^2}\left(\frac{d_{Si}'}{k_{Si}} + \frac{d_{Cr}}{k_{Cr}} + \frac{d_g}{k_g}\right) + \frac{L_H}{\pi R_H^2 k_H} \qquad (1)$$

Where,

$$R_{Si} = \frac{1}{\pi}\sum_{i=0}^{n-1}\left[\frac{W}{r_i^2 k_{Si}}\right] = \textit{Thermal resistance of p-Layer},$$

$$(r_{i+1} - r_i) = \frac{(r_{n-1} - r_0)}{(n-1)} \text{ for } [0 \le i \le (n-2)]\ ,\ W = \frac{d_{Si}}{n}.$$

Similarly the Total thermal resistance of the ring diode [below the junction] along with the heat sink is calculated using (2) keeping in mind the above assumptions,

$$Rth = RSi + \frac{1}{\pi r_{n-1}'^2}\left(\frac{d_{Si}'}{k_{Si}} + \frac{d_{Cr}}{k_{Cr}} + \frac{d_g}{k_g}\right) + \frac{L_H}{\pi R_H^2 k_H} \qquad (2)$$

Where,

$$R_{Si} = \frac{1}{\pi}\sum_{i=0,\,j=0}^{n-1,n-1}\left[\frac{W}{\left(r_i^{'2} - r_j^{''2}\right)k_{Si}}\right] = \textit{Thermal resistance of p-Layer},$$

$$\left(r_{i+1}^{'} - r_i^{'}\right) = \frac{\left(r_{n-1}^{'} - r_0^{'}\right)}{(n-1)} \text{ for } [0 \le i \le (n-2)],$$

$$\left(r_j^{''} - r_{j+1}^{''}\right) = \frac{\left(r_0^{''} - r_{n-1}^{''}\right)}{(n-1)} \text{ for } [0 \le j \le (n-2)],\ W = \frac{d_{Si}}{n}$$

Junction temperatures are calculated using (3). Where diode efficiency (η), breakdown voltage (V_{dc}), and bias current density (J_{dc}) are taken from first row of Table 2. Thermal resistance values for both the diodes along with heat sinks are available in Table 5 calculated from (1) & (2). Effective junction area (A_{eff}) of both type of diodes [Mesa & Ring] are assumed as equal [i.e. $A_{eff} = \pi r_0^2 = \pi(r_0^{'2} - r_0^{''2})$].

Actually the heat sink (diamond and copper) dimensions for both type diodes are chosen in such a way that junction temperatures at steady state for both the diode structures remain almost equal.

$$T_j = [300 + R_{th}(1-\eta)V_{dc}J_{dc}A_{eff}] \qquad (3)$$

1. Finite Difference Method

In this section a brief of Finite Difference Method is given [8]. Consider a two dimensional body which is to be divided into equal increments in both the ‘x’ and ‘y’ directions, as shown in Figure 3. The nodal points are designated as shown, the ‘m’ locations indicating the ‘x’ increment and ‘n’ locations indicating the ‘y’ increment. We wish to establish the temperatures at any of the nodal points within the body, using (4) as a governing condition.

$$\frac{\partial^2 T}{\partial x^2} + \frac{\partial^2 T}{\partial y^2} = 0 \qquad (4)$$

Finite differences are used to approximate differential increments in the temperature and space coordinates; and the smaller we choose these finite increments, the more closely the true temperature distribution will be approximated.

4.1) Interior node: For any interior node (m,n) as shown in the Figure 3 for square grids [$\Delta x = \Delta y$] we can determine the temperature of that node, $T_{m,n}$ from the knowledge of surrounding 4 node temperatures by (5) in Table 3. Since we are considering the case of constant thermal conductivity, the heat flows may all be expressed in terms of temperature differentials. Equation (5) in Table 3 states very simply that the net heat flow into any node is zero at steady-state conditions. In effect, the numerical finite-difference approach replaces the continuous temperature distribution by fictitious heat-conducting rods connected between small nodal points which do not generate heat. To utilize the numerical method, (5) in Table 3 must be written for each node within the material and the resultant system of equations solved for the temperatures at the various nodes.

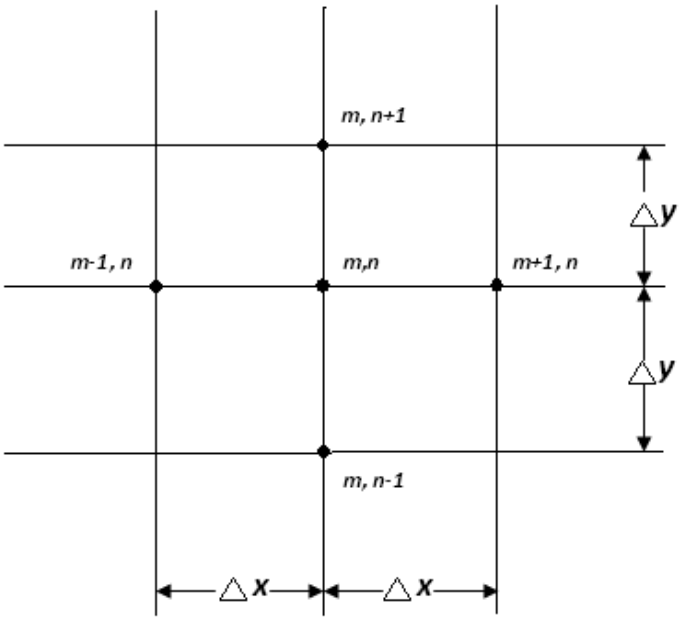

Figure 3: Sketch illustrating nomenclature used in two-dimensional numerical analysis of heat conduction.

4.2) Convection boundary node: When solid is exposed to some convection boundary condition, the temperatures at the surface must be computed differently from the method given above. For any convection boundary node (m,n) as shown in the Figure 4 for square grids [$\Delta x = \Delta y$] we can determine the temperature of that node, $T_{m,n}$ from the knowledge of surrounding 3 node temperatures along with the ambient temperature [T_∞=300 K] by (6) in Table 3. Here, h = Convection heat-transfer Coefficient. An equation of this type must be written for each node along the surface shown in Figure 4. So when a convection boundary is present, an equation like (6) in Table 3 is used at the boundary and an equation like (5) in Table 3 is used for interior points.

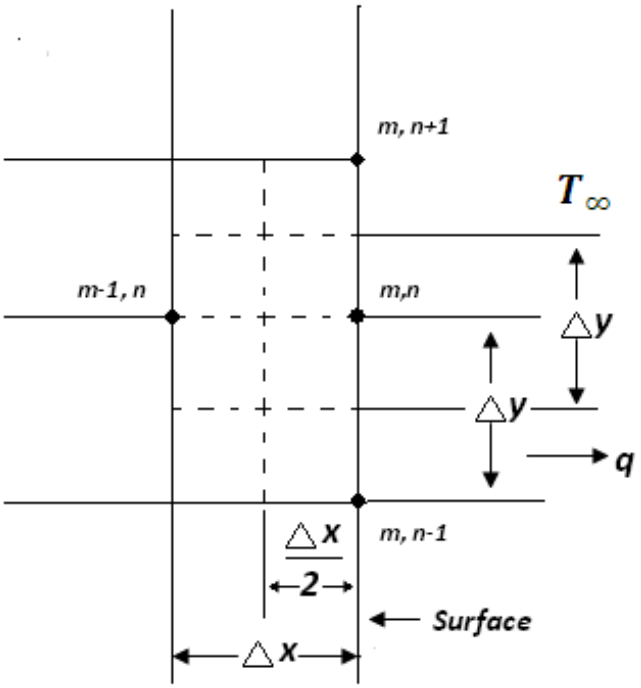

Figure 4: Sketch illustrating nomenclature for nodal equation with convection boundary conduction.

4.3) Exterior Corner with Convection Boundary: Consider a exterior corner section shown in Figure 5. For any corner node (m,n) convection boundary as shown in the Figure 5 for square grids [$\Delta x = \Delta y$] we can determine the temperature of that node, $T_{m,n}$ from the knowledge of surrounding 3 node temperatures along with the ambient temperature [T_∞ = 300 K] by (7) in Table 3.

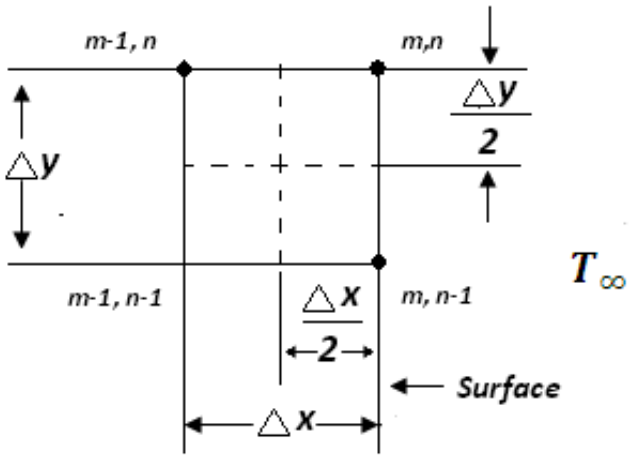

Figure 5. Sketch illustrating nomenclature for nodal equation with convection at a Corner Section.

Table 3. Summary of the FDM Nodal Equations

PHYSICAL SITUATION	NODAL EQUATION FOR EQUAL INCREMENTS IN 'x' AND 'y'
1. Interior node	$T_{m,n} = \left[\frac{T_{m+1,n} + T_{m-1,n} + T_{m,n+1} + T_{m,n-1}}{4}\right]$ (5)
2. Convection Boundary node	$T_{m,n} = \frac{\left[T_{m-1,n} + \frac{[T_{m,n+1} + T_{m,n-1}]}{2}\right] + BiT_\infty}{[2+Bi]}$ (6)
	Where, $Bi = h\frac{\Delta x}{k}$
3. Exterior Corner with Convection Boundary	$T_{m,n} = \frac{\left[\frac{T_{m-1,n} + T_{m,n-1}}{2}\right] + BiT_\infty}{[1+Bi]}$ (7)
	Where, $Bi = h\frac{\Delta x}{k}$

RESULTS AND DISCUSSION

For proper operation of the diodes during continuous wave steady state operation heat sinks must be accurately designed to avoid the burn-out of the device. The burn-out temperature of

Silicon is 575 K. So the total thermal resistance of the diode and heat sink must have such a value that will able to keep the junction temperature [can be calculated using (3)] well below the burn-out temperature of Silicon. So heat sink dimensions are chosen such a way that the total thermal resistance would obtain that desired value which actually capable of keeping the junction temperature below 575 K.

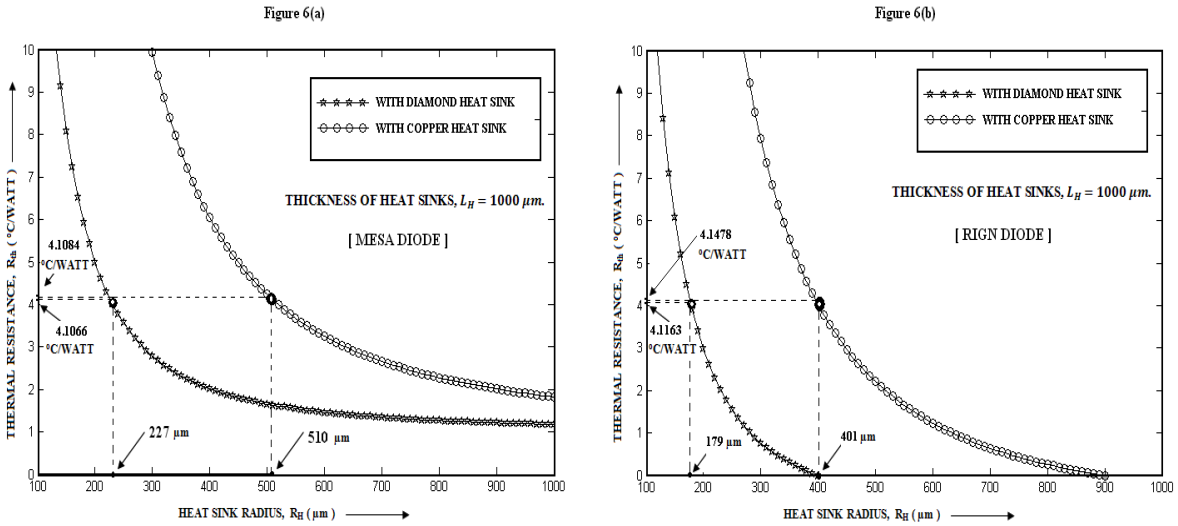

Figure 6(a) & (b): Total Thermal Resistance Vs Heat Sink Radius plots for Mesa and Ring Diodes.

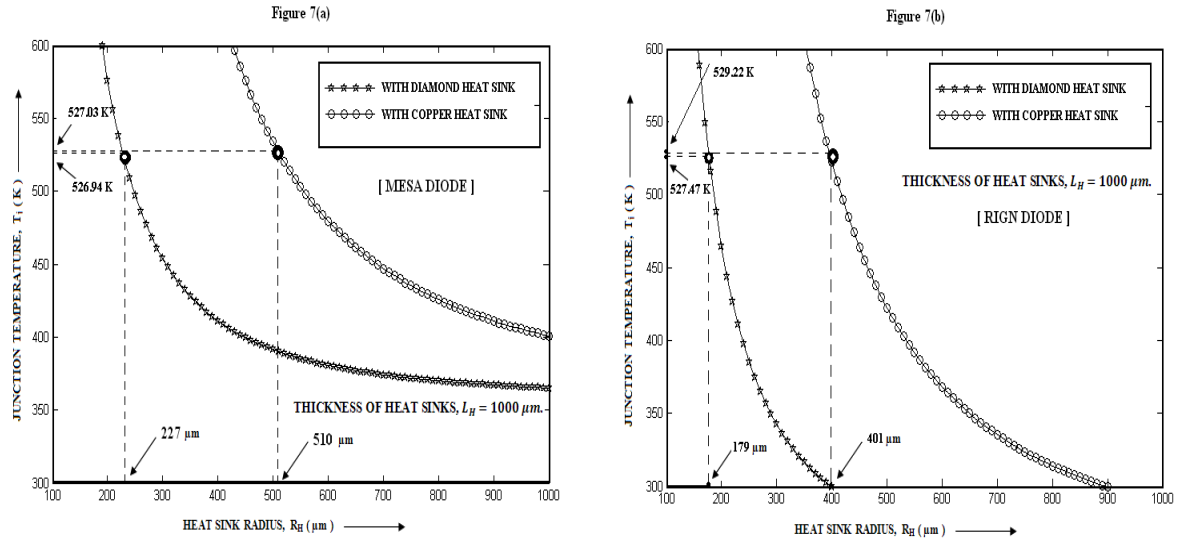

Figure 7(a) & (b): Junction Temperature Vs Heat Sink Radius plots for Mesa and Ring Diodes.

Firstly we have plotted total thermal resistances (1) & (2) [for mesa and ring diodes respectively] against heat sink radius keeping the thickness of the heat sinks fixed at 1000 µm [for both diamond and copper]. That plots are shown in Figure 6(a) & (b). From the plots we have chosen the radius values of heat sinks such a way that, those dimensions of the heat sinks provide the desired values of total thermal resistances those are capable of keeping junction temperatures well below the burn out temperature of Silicon [T_B = 575 K]. Junction temperature vs heat sink radius plots are shown in Figure 7 (a) & (b) for mesa and ring diodes respectively. Optimum heat

sink radius values are also indicated on all those plots.

Designed heat sink (made of diamond and copper) dimensions are tabulated in Table 4 for both structures of the diodes (mesa and ring). These dimensions are obviously the optimum dimensions of the heat sinks [diamond and copper] for both types of diodes [mesa and ring] for the safe and steady operation of the oscillators at continuous wave mode capable of avoiding the device burn-out.

Table 4. Dimensions of the Designed Heat Sinks

DIMENSIONS	MESA DIODE		RING DIODE	
	DIAMOND	COPPER	DIAMOND	COPPER
RADIUS, R_H (μm)	227	510	179	401
THICKNESS, L_H (μm)	1000	1000	1000	1000

Table 5. Total Thermal Resistances and Junction Temperatures

PARAMETERS	MESA DIODE		RING DIODE	
	DIAMOND	COPPER	DIAMOND	COPPER
TOTAL THERMAL RESISTANCE, R_{th} (^oC/Watt)	4.1066	4.1084	4.1163	4.1478
JUNCTION TEMPERATURE, T_j (K)	526.94	527.03	527.47	529.22

Calculated Total thermal resistances and junction temperatures for both the diode structures and for both diamond and copper heat sinks are listed in Table 5. We can observe from Table 5 that the junction temperatures are now well below the burn-out temperature of the Silicon [i.e. $T_j < T_B = 575$ K]. So the heat sinks are designed properly for the safe operation. To find out the effective area of the diode junctions (A_{eff}), we have taken junction radius of mesa diode, $r_0 = 40$ μm and for ring diode the outer junction radius is, $r_0' = 50$ μm and inner junction radius is, $r_0'' = 30$ μm. Actually the effective junction areas (A_{eff}) of both type of diodes [Mesa and Ring] are equal in this case. Also we have taken 'n = 100' for both the mesa and ring diodes to get appreciable accuracy.

Now the Finite Difference Method [FDM] described in the earlier section is used to find out the temperature distribution inside the diodes (both mesa and ring structures) and heat sinks. Diodes and heat sinks are of having circular cross sections, maintaining the symmetrical structures. Thus due to symmetrical shapes, in cylindrical co-ordinate system (r,ɵ,z) we can eliminate the 'ɵ' co-ordinate for simplicity. Now these can be considered as two dimensional temperature distribution problems. So, in case of rectangular co-ordinate system (x,y,z) we have to consider only 'x' and 'y' co-ordinates; here we can eliminate the 'z' co-ordinate. That is why we have taken the two dimensional Laplace Equation (4) as governing condition of our FDM analysis. So, it is sufficient to get 2-D solution of (4) for getting complete temperature distribution for these symmetrical structures.

As we know that the diode dimensions are much smaller than that of heat sinks, so if we show the temperature distribution plots of a diode and heat sink together in a single plot then it will be very much difficult to recognize the temperature variations inside that diode (due to its smaller size). That is why we have shown the temperature distributions inside the diodes and heat sinks

separately. First let us consider the case of mesa diode on semi-infinite diamond and copper heat sink separately. Figure 1(a) shows that it is a symmetrical structure. So 2-D temperature distribution analysis is enough to describe the thermal distribution inside the entire structure completely, as discussed previously. The whole structure (from below the p-n junction) is divided into a number of intersecting horizontal and vertical grids having the same distance between any two consecutive nodes (described in Section 4, i.e. $\Delta x = \Delta y$). At the junction we have assumed that the junction temperature (given in Table 5) is distributed uniformly. Every node at the junction has the same temperature values that are equal to the junction temperature. The every node at side walls of both the diode and heat sink and the lower surface of the heat sink nodes are taken as convection boundary nodes with, $T\infty = 300K$ = Temperature of the ambient. Now using the above assumptions and using TABLE III we have written a MATLAB program which is actually capable of developing simultaneous FDM nodal equations. These simultaneous nodal equations are solved by Gauss-Seidel Iterative method. After getting the solutions, now the temperatures of each node are available. Normalized values of temperatures are plotted with respect to the normalized radius vector for diode and heat sinks separately in Figure 8 and Figure 9(a) & (b) respectively. Temperatures are normalized with respect to junction temperature and radius values are normalized with respect to diode radius at diode heat sink interface [R = 100 μm, for both Mesa and Ring Diodes].

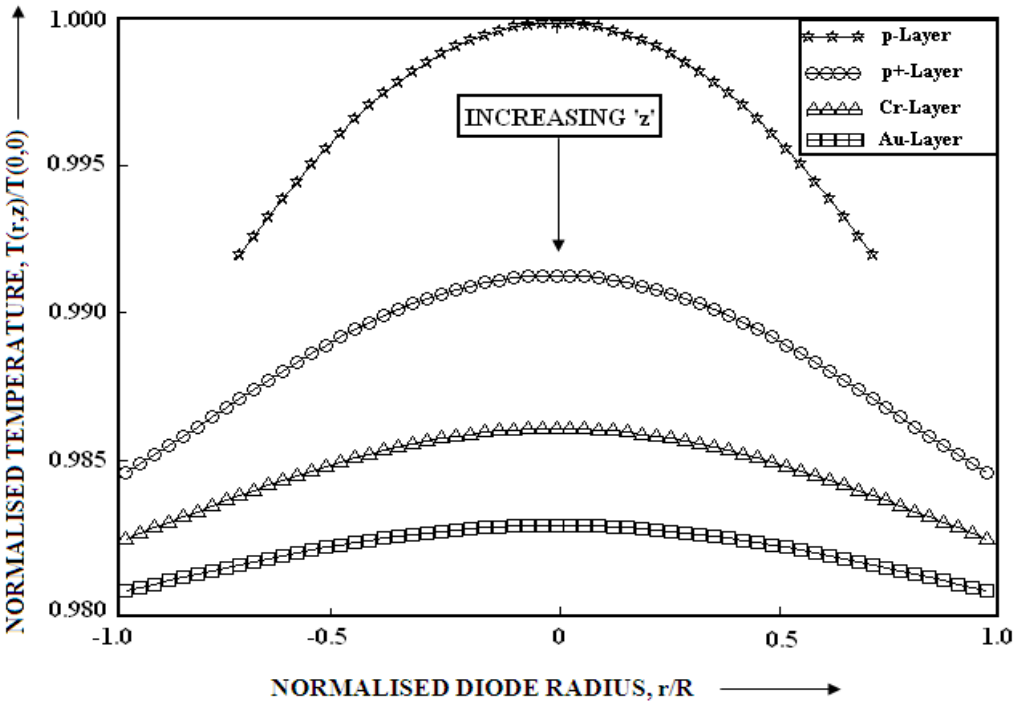

Figure 8: Normalized Temperature Distribution inside the Mesa Diode [*T(r,z)/T(0,0) Vs r/R*], *R = 100* μm and *T(0,0) = T_j*.

The same methods are applied to the ring diode along with the heat sink [diamond and copper] and the associated plots are shown in the Figure 10 [Diode] and Figure 11 (a) & (b) [Heat Sinks]. It can be observed from Figure 8 and Figure 10 that the fall of temperatures at the diode-heat sink interfaces are very less with respect to the junction temperatures.

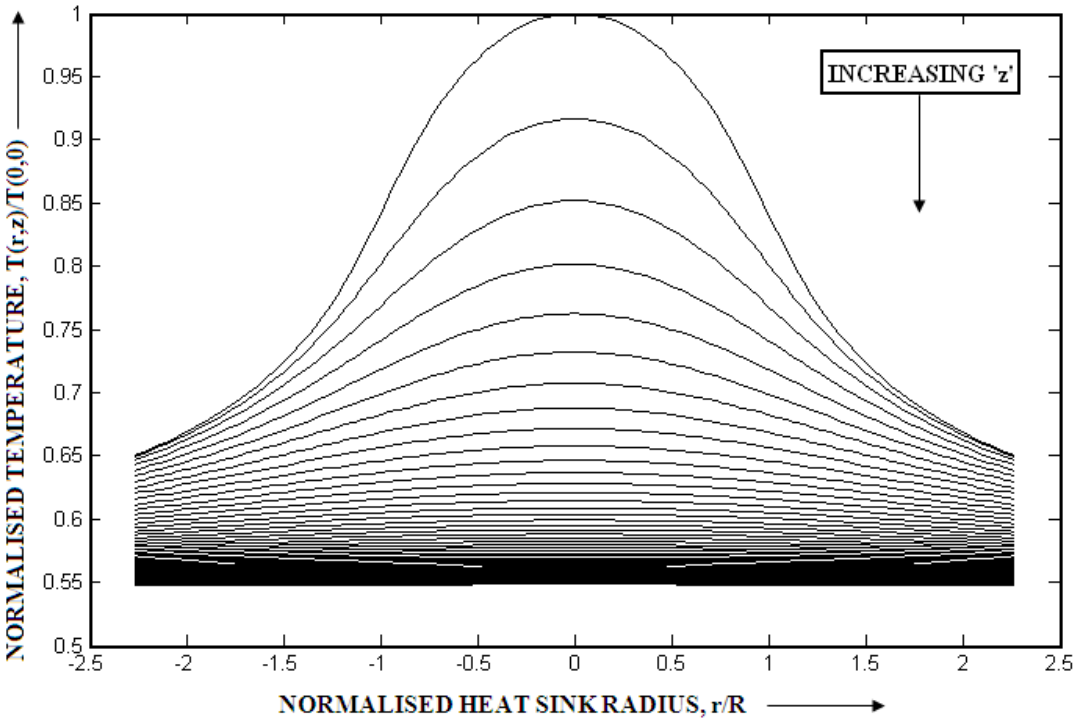

Figure 9(a): Normalized Temperature Distribution [For Mesa Structure] inside the Diamond Heat Sink [*T(r,z)/T(0,0) Vs r/R*], R = 100 µm and *T(0,0)* = T_j.

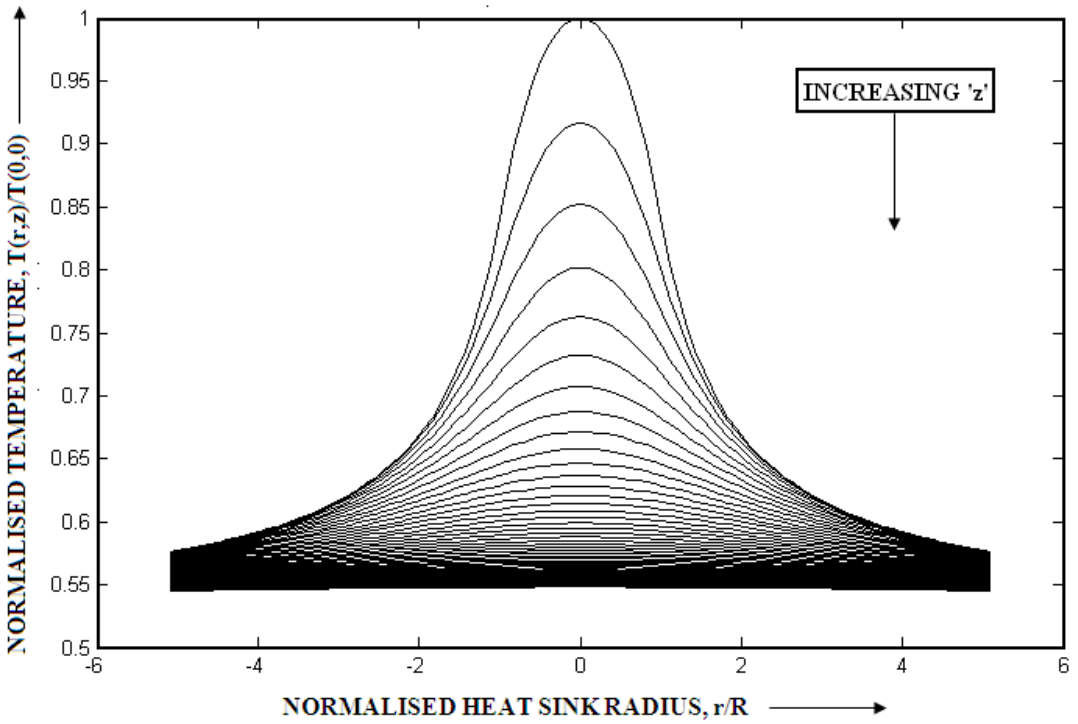

Figure 9(b): Normalized Temperature Distribution [For Mesa Structure] inside the Copper Heat Sink [*T(r,z)/T(0,0) Vs r/R*], *R = 100 µm* and *T(0,0)* = T_j.

Those are because thermal conductivities of the materials of different diode layers are not so high (k_{Si} = 80 watt/m ^oC, k_{Cr} = 93.9 watt/m ^oC, k_{Au} = 320 watt/m ^oC) and more importantly the thicknesses of those layers are also very small (Actually the total diode thicknesses are very small below the junction). But the thermal conductivities of Diamond and Copper (mentioned

earlier) are very high. And the heat sinks are designed such a way that temperature at the lower surfaces of those fall to ambient temperature (300 K) during steady state of operation. Diamond heat sinks require much less dimensions than copper heat sinks because at about 500 K the thermal conductivity of diamond is almost five times larger than copper.

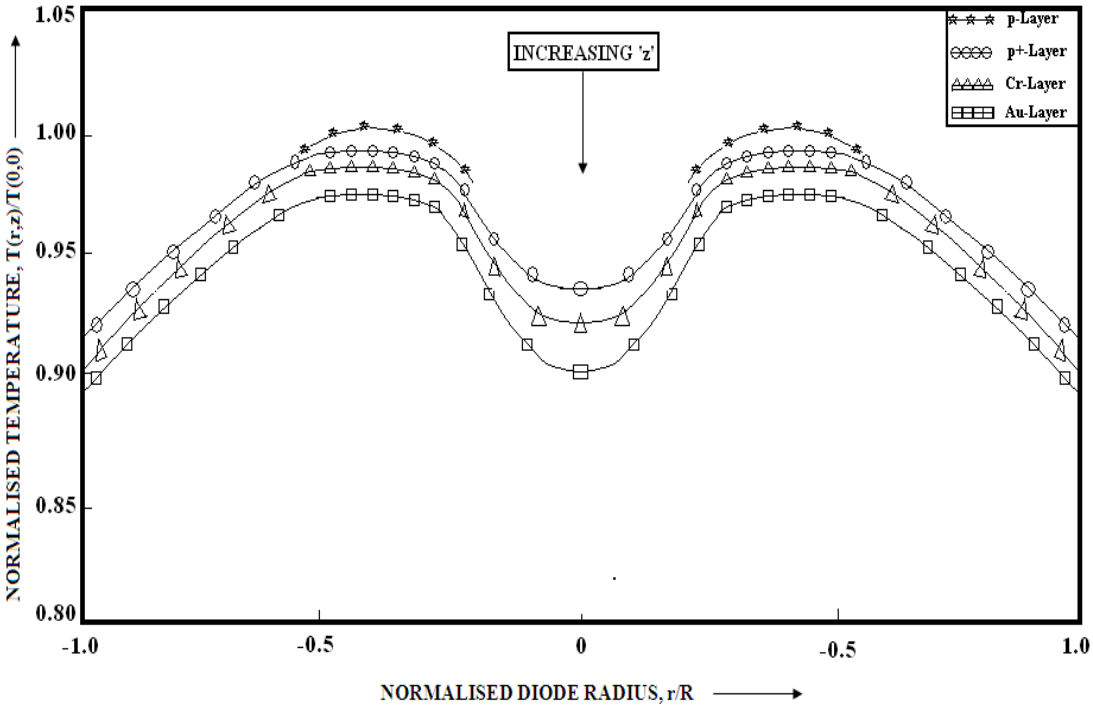

Figure 10: Normalized Temperature Distribution inside the Ring Diode [*T(r,z)/T(0,0) Vs r/R*], *R = 100 µm* and *T(0,0) = T_j*.

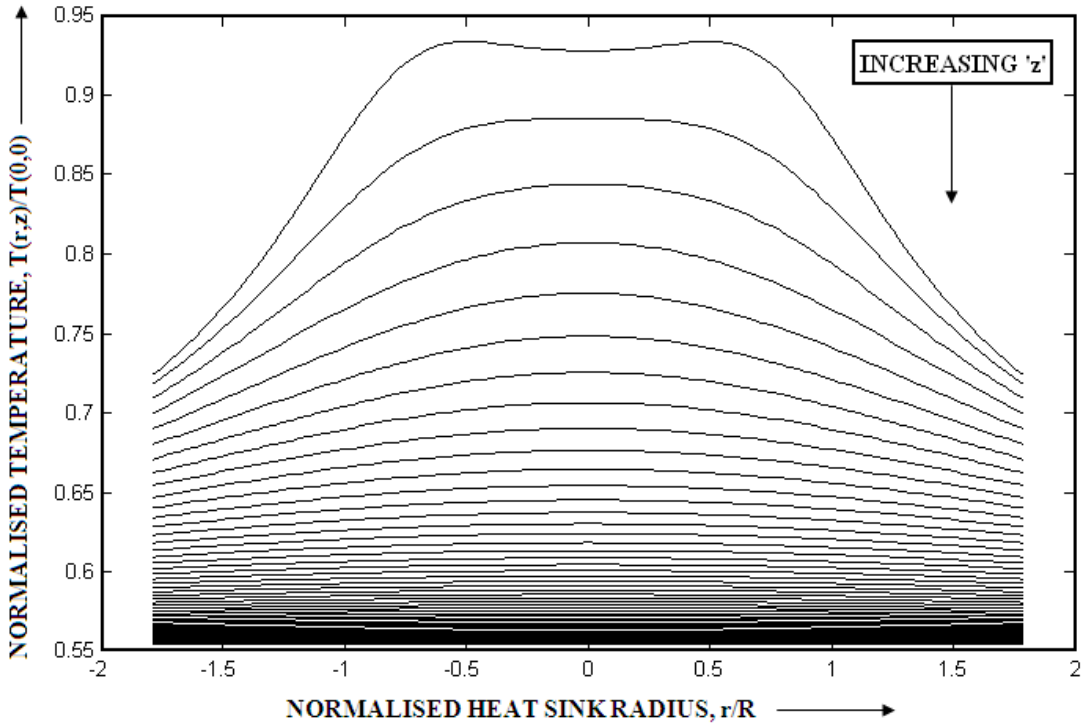

Figure 11(a). Normalized Temperature Distribution [For Ring Structure] inside the Diamond Heat Sink [*T(r,z)/T(0,0) Vs r/R*], *R = 100 µm* and *T(0,0) = T_j*.

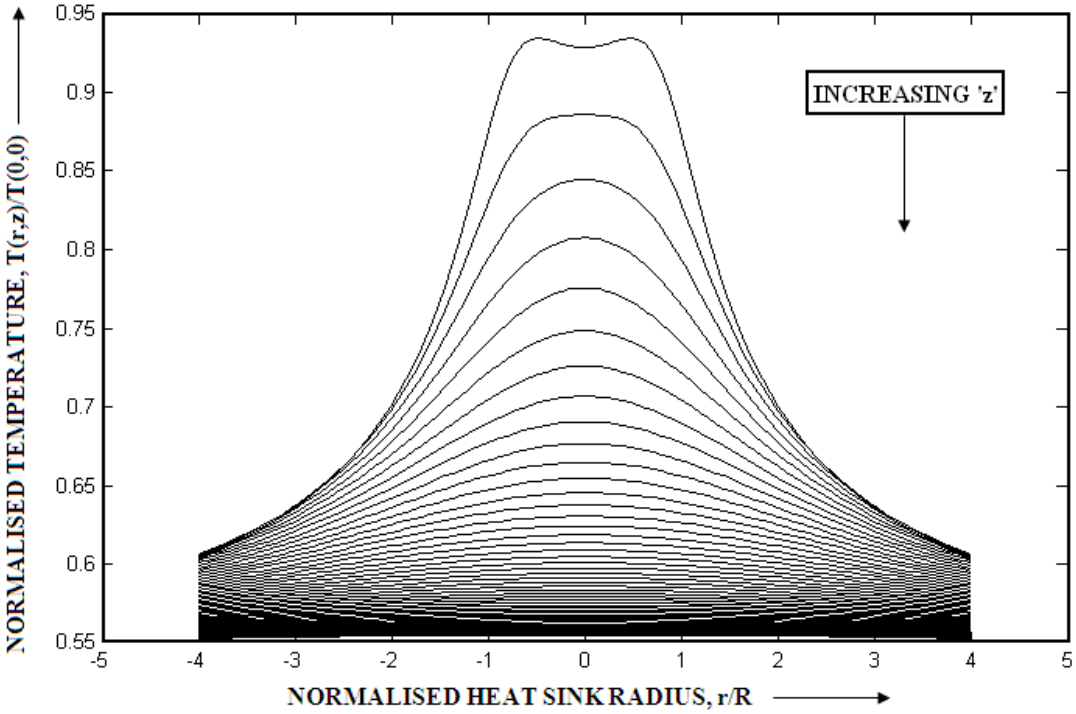

Figure 11(b): Normalized Temperature Distribution [For Ring Structure] inside the Copper Heat Sink [*T(r,z)/T(0,0) Vs r/R*], *R = 100 μm* and *T(0,0) = T_j*.

CONCLUSION

A novel method of getting optimum design for IMPATT diode oscillator heat sinks is presented here. Accurate formulation of total thermal resistances for both mesa and ring structures mounted on semi-infinite heat sinks are given here. Accuracy in determination of total thermal resistances actually provides accurate and optimum design of heat sinks for steady and safe operation of IMPATT oscillators in continuous wave mode which is capable of avoiding burn-out phenomena. Keeping in mind the cost of the system, typical equivalent heat sink designs are presented in this paper by using both diamond [High Cost] and copper [Comparatively Low Cost].

In many practical steady state heat transfer problems the geometry or boundary conditions are such that an analytical solution has not been obtained at all, or if the solution has been developed, it involves such a complex series solution that numerical evaluation becomes exceedingly difficult. For such cases the most useful approach to the problem is one based on Finite-Difference Method [FDM] to easily find out the Temperature Distribution. So we have applied Finite-Difference Method to find out 2-D Temperature Distribution inside the mesa and ring diodes mounted on semi-infinite diamond and copper heat sinks. Solutions are totally similar with the analytical solutions [2] except errors associated with FDM. Non-uniform temperature distribution inside the diodes causes non-uniform current distribution also. It might be expected that the large variation in current density in the solid mesa diode and in ring diode would have a measurable effect on the microwave performance of the IMPATT oscillator. In particular properties like efficiency, noise and electronic tuning sensitivity could be affected by the non-uniform current distribution. So our proposed method of finding temperature distribution inside the diodes will be very useful and easier way to find out current distribution inside the diode also [3]. After getting the current distribution now it will be very easy to investigate its

effect on various millimeter-wave properties of IMPATT oscillator.

REFERENCES

[1] B. Pal, A. Acharyya, A. Das, J. P. Banerjee, *Proceedings of National Conference on MDCCT 2010, Burdwan*, **2010**, p. 58-59.
[2] A. Acharyya, B. Pal, J. P. Banerjee, *International Journal of Electronic Engineering Research*, **2010**, vol 2, no. 4, pp. 553-567.
[3] G. Gibbons, T. Misawa, *Solid State Electron.*, **1968**, vol. 11, p. 1007.
[4] D. P. Kennedy D, *J. Appl. Phys.*, **1960**, vol. 31, p. 1490.
[5] H. S. Carslaw, J. C. Jaeger, Conduction of Heat in Solids, Oxford: Clarendon, **1959**.
[6] J. Frey, *IEEE Trans. Electron Devices*, **1972**, vol. ED-19, p. 981.
[7] R. L. Bernick, *Electronic Letters*, **1972**, vol. 8, no. 7, p. 180.
[8] J. P. Holman, Heat Transfer, Tata McGraw Hill [Ninth Edition].
[9] G. Gibbons G, Clarendon Press, Oxford, **1973**.
[10] A. Acharyya, J. P. Banerjee, *International Journal of Engineering Science and Technology*, **2011**, vol. 3, no. 1, pp. 332-339.